

# Determining the spectroscopic mass ratio in interacting binaries: Application to X-Ray Nova Sco 1994

T. Shahbaz

*Instituto de Astrofísica de Canarias E-38200 La Laguna, Tenerife, Spain*

30 October 2018

## ABSTRACT

We present a model for determining the mass ratio in interacting binaries by directly fitting the observed spectrum with synthetic spectra. We make direct use of NEXTGEN model atmospheres intensities which are the most comprehensive and detailed models available for cool stars. We fully take into account the varying temperature and gravity across the secondary star’s photosphere, by incorporating the synthetic spectra into the secondary star’s Roche geometry. As a result, we determine the exact rotationally broadened spectrum of the secondary star and so eliminate the need for a limb-darkening law, and the uncertainties associated with it.

As an example we determine the mass ratio for the well studied soft X-ray transient Nova Sco 1994. In order to obtain a more accurate determination of the mass ratio, which does not depend on assumptions about the rotation profile and limb-darkening coefficients, we use our model to compute the exact rotationally broadened model spectrum, which we compare directly with the observed intermediate resolution spectrum of Nova Sco 1994. We determine the mass ratio of Nova Sco 1994 to be  $0.419 \pm 0.028$  (90 percent confidence), which is the most accurate determination of the binary mass ratio in an X-ray binary. This result combined with the binary mass function and inclination angle gives a refined black hole mass of  $5.99 \pm 0.42 M_{\odot}$  (90 percent confidence). We also perform simulations which show that, for an F-type secondary star, the standard rotation profile with zero and continuum value for the line limb-darkening coefficient gives a value for  $q$  that brackets the value found using the full geometrical treatment

**Key words:** binaries: – close – stars: fundamental parameters, individual: X-Ray Nova Sco 1994 (GRO J1655–40) – X-rays: stars

## 1 INTRODUCTION

The determination of binary masses in interacting binaries where only one component is observable, such as in cataclysmic variables (CVs) or low-mass X-ray binaries (LMXBs), requires a radial velocity study of the mass loosing star, a knowledge of the binary inclination angle and mass ratio. The binary inclination in non-eclipsing binaries is usually obtained by measuring the ellipsoidal modulation of the late-type star (e.g. see Wilson & Devinney 1971 and Shahbaz, Naylor & Charles 1993) and the binary mass ratio is normally obtained by measuring the rotational velocity of the secondary star (Wade & Horne 1988). This procedure has been used for many years to determine binary masses, in particular in the subclass of the LMXBs called the soft X-ray transients (SXTs), which are characterised by their episodic outbursts and contain some of the best stellar mass black hole candidates (van Paradijs & McClintock 1995).

It is clear that if one wants to determine accurate binary masses for the SXTs, the uncertainties in measuring the inclination angle and mass ratio have to be reduced. This paper concentrates on reducing the inherent uncertainties associated in determining the binary mass ratio.

Shahbaz (1998) showed that in principle, one could use the shape of the secondary star’s absorption lines to determine the binary system parameters, such as the inclination angle. However, this requires high resolution echelle spectroscopy, which for most of the faint SXTs is very difficult, even with 10-m class telescopes. Due to the faintness of the secondary star in the SXTs, the secondary star’s rotational broadening is usually determined by using intermediate resolution ( $\sim 1\text{\AA}$ ) spectroscopy. The secondary stars typically have  $V_{\text{rot}} \sin i$  values of 30–100 km/s. With intermediate resolution spectroscopy the information about the shape of the absorption lines is lost, the only information that can be extracted is the amount by which the star’s spectrum is

broadened. The procedure commonly used to measure the secondary star rotational broadening is to compare it with the spectrum of a slowly rotating template star, observed with the same instrumental configuration which has been convolved with a limb-darkened standard rotation profile (Gray 1992; Collins & Truax 1995 and references within). For this one needs to assume a limb-darkening coefficient for each spectral line. Usually one either adopts 0, i.e. no limb darkening, or the continuum value (which depends on the wavelength and the star's effective temperature). The width of the standard rotation profile is varied until an optimum match is found with the width of the target spectrum (e.g. see Marsh, Robinson & Wood 1994).

It should be noted that there are many assumptions inherent in using this method, primarily due to the use of the standard rotation profile. The standard rotation profile assumes that the star is spherical and that the line profile has the same shape over the entire star. It also assumes a wavelength dependent limb darkening coefficient and a homogeneous stellar surface. Firstly, it should be noted that the secondary star in a CV or LMXB substantially fills its Roche lobe so is far from being spherical and will thus have distorted line profiles the extent of which depends on the exact Roche geometry (Shahbaz 1998). Also, the spectrum of the secondary cannot be described by a single-star spectrum, since both temperature and gravity vary over the photosphere due to the shape of the star's Roche-lobe. Furthermore, stellar absorption lines have core limb-darkening coefficients much less than the appropriate continuum value because the line flux arises from higher regions in the stellar atmosphere than the continuum flux; the precise value for the line limb-darkening coefficient depends on many parameters such as the incidence angle and so requires detailed calculations (Collins & Truax 1995). Using zero or the continuum value introduces a systematic uncertainty of about 14 percent in the determination of  $V_{\text{rot}} \sin i$  (Welsh et al., 1995, Shahbaz 1998) which contributes significantly to the accuracy which one can determine the mass ratio and hence the binary masses.

In an attempt to reduce the uncertainties in the binary mass ratio derived from intermediate spectroscopy using this procedure, we determine the exact rotationally broadened spectrum from the secondary star in an interacting binary. Our calculations take into account the shape of the secondary star's Roche-lobe and the varying temperature and gravity of different photospheric segments, which are characterised by individual model atmospheres. By directly comparing the model spectrum with the observed intermediate resolution spectra of an SXT, we show that we can accurately determine the binary mass ratio. As an example, we determine the binary mass ratio for the well studied soft X-ray transient, Nova Sco 1994 (=GRO J1655-40).

## 2 DETERMINING THE SPECTRUM IN INTERACTING BINARIES

Although there are many codes that use model atmospheres to determine the light curves of binary systems (Wilson & Devinney 1971, Tjemkes, van Paradijs & Zuiderveld 1986, Shahbaz et al., 1993, Orosz & Hauschildt 2000) there are not many that compute the observed spectrum. Linnell &

Hubeny (1994, 1996) have a code that computes the synthetic spectra and light curves for binary stars. However, since they use Kurucz (1979) model atmospheres to synthesize the spectrum, their code is really only applicable for systems with relatively hot stellar components i.e. early-type stars. In LMXBs, the low-mass companions are typically late-type K stars with effective temperatures less than 5000 K. Also, since the temperature varies across the star's surface due to gravity darkening, there are elements on the star's surface much cooler than the star's effective temperature, especially near the inner Lagrangian point ( $L_1$ ; Shahbaz 1998). Therefore, in order to compute the observed spectrum of the late-type secondary star in an LMXB accurately and to make the code more general for a range of secondary stars, we have written a code that is similar to the code used in Shahbaz (1998) but with a full treatment of limb darkening through the addition of synthetic NEXTGEN model atmospheres.

## 3 THE MODEL

The equations that determine the basic geometry of an interacting binary system have been known for a long time and are well understood. To determine the light curve or spectrum from the secondary star in a close binary, one would compute the specific intensity for each element of area on the star's surface by solving the radiation transfer equation for a given model photosphere. By doing this one eliminates the need to use a limb-darkening law which parameterizes the specific intensity for different emergent angles, given the monochromatic intensity. However, since the computation of stellar atmospheres is computationally intensive, approximations are required to determine the expected light curve or spectra from an interacting binary system.

The main geometrical part of the model we use is the same as that described in Shahbaz (1998) and is similar to other standard models for interacting binaries (Tjemkes et al., 1986, Orosz & Bailyn 1997). Briefly, we model a binary system in which the primary is a compact invisible object and the secondary a "normal" star. We assume that the secondary fills its Roche-lobe, is in synchronous rotation and has a circular orbit. A grid consisting of a series of quadrilaterals of approximately equal area is set up over the Roche surface. The grid is defined using a polar coordinate system with  $N_\theta$  rings equally spaced across the star, from the  $L_1$  point to the back of the secondary star (see Orosz & Bailyn 1997 for details). For each ring of constant angle  $\theta$  the number of azimuth points is chosen to try to keep the area roughly constant. We typically use  $N_\theta=40$ , which corresponds to 2048 surface elements.

The parameters that determine the geometry of the system are the binary inclination  $i$ , the binary mass ratio  $q$  ( $=M_2/M_1$ , where  $M_1$  and  $M_2$  are the masses of the compact object and secondary star respectively) and the Roche-lobe filling factor,  $f$ . Since we assume the secondary fills its Roche-lobe, a safe assumption in LMXBs,  $f=1$ . The radial velocity semi-amplitude,  $K_2$ , determines the velocity scale of the system. The velocity, gravity and temperature for each element varies across the star due to the shape of the Roche-lobe, the Roche-potential and gravity darkening respectively. The temperature and gravity for each element

**Table 1.** SXTS with spectroscopic mass ratio measurements

Object	$V_{\text{rot}} \sin i$ (km/s)	$q (= M_2/M_1)$	Reference
GRO J0422+32	$90^{+22}_{-27}$	$0.116^{+0.079}_{-0.071}$	Harlaftis et al., (1999)
A0620-00	$83 \pm 5$	$0.067 \pm 0.01$	Marsh, Robinson & Wood (1994)
GS2000+25	$86 \pm 8$	$0.042 \pm 0.012$	Harlaftis, Horne & Filippenko (1996)
Nova Mus 1994	$106 \pm 13$	$0.128^{+0.044}_{0.039}$	Casares et al., (1997)
Cen X-4	$43 \pm 6$	$0.17 \pm 0.06$	Torres et al., (2002)
XTE J1550-564	$90 \pm 10$	$0.152^{+0.048}_{0.042}$	Orosz et al., 2002
Nova Sco 1994	$82.9$ – $94.9$	$0.337$ – $0.436$	S99
V4641 Sgr	$123 \pm 4$	$0.667 \pm 0.356$	Orosz et al., 2001
V404 Cyg	$39.1 \pm 1.2$	$0.060^{+0.004}_{-0.005}$	Casares & Charles (1994)

are scaled using the observed effective temperature  $\langle T_{\text{eff}} \rangle$  and gravity  $\langle \log g \rangle$ , which is determined from the spectral type and class of the secondary star.

The local gravity is scaled so that the integrated gravity over the star surface is given by the observed gravity. The temperature of each element is calculated using the well-known von Zeipel relation (von Zeipel 1924),  $T \propto g^\beta$  where  $\beta$  is the gravity darkening exponent, and is scaled so that the integrated luminosity over the stellar surface matches the observed bolometric luminosity. The limb angle  $\mu = \cos \theta$ , is the angle between the local surface normal and the line of sight to the observer;  $\mu=1$  at the center of the star and  $\mu=0$  at the limb. Each element of area on the surface of the star is assigned a temperature, gravity, projected velocity and limb angle  $\mu$ . For a fixed wavelength, the specific intensity for a given element of area depends on  $T_{\text{eff}}$ ,  $\log g$  and  $\mu$ .

### 3.1 The synthetic spectra

To compute the specific intensity at a given wavelength we use the multi-purpose state-of-the-art stellar atmosphere code PHOENIX, which produces NEXTGEN model atmospheres, the details of which can be found in Hauschildt, Baron & Allard (1997) and Hauschildt et al., (1999). The NEXTGEN models are the most detailed models available for cool stars and are computed using spherical geometry, rather than the usual plane-parallel approximation. Since computing NEXTGEN models are heavily time consuming, we cannot compute spectra for all effective temperatures, gravities and limb angles. Therefore, we precompute spectra for set  $T_{\text{eff}}$ ,  $\log g$  and  $\mu$  combinations.

We compute model spectra with solar abundance in the wavelength range 6300 to 6800 Å in steps of 0.1 Å  $T_{\text{eff}}$  in the range 2400 K to 9800 K in steps of 200 K and  $\log g$  in the range 1.5 to 5.0 in steps of 0.5. The wavelength range above was chosen because this region is commonly used to determine the secondary star's rotational broadening since it has many strong Fe and Ca absorption line features intrinsic to late-type stars. For a given  $T_{\text{eff}}$  and  $\log g$ , PHOENIX computes the specific intensities for 64 different angles which are chosen by the code based on the structure of the atmosphere. For consistency between the models we interpolate the specific intensities onto a regular grid with  $\mu$  values ranging from 0.05 to 1.0. For accuracy we use a spline interpolation method (Press et al., 1992) in logarithmic units. Also, we set the specific intensity to be zero for  $\mu < 0.05$ , since at such high limb angles the specific intensity is negligible (see

Orosz & Hauschildt 2000 for details). Finally, to determine the specific intensity for a given wavelength we perform a 3-D logarithmic interpolation in  $T_{\text{eff}}$ ,  $\log g$  and  $\mu$  (see section 3.2).

For each element of area visible we compute  $T_{\text{eff}}$ ,  $\log g$  and  $\mu$ . We then determine the specific intensity at each specified wavelength and integrate the visible specific intensity values over the Roche surface. We velocity-correct the model spectra by first converting the wavelength scale from vacuum to air (Allen 1973) and then bin the spectra onto a uniform wavelength scale. Finally, given a colour excess we redden the spectrum using the reddening law from of Seaton (1979). We thus obtain the exact rotationally broadened spectrum of the secondary star at a given orbital phase. The model parameters that determine the width and shape of the model absorption lines are  $q$ ,  $i$ ,  $K_2$  and  $\beta$ ;  $q$  and  $K_2$  determine primarily determine the width of the lines, whereas  $i$  and  $\beta$  mainly determine the shape of the absorption line (also see Shahbaz 1998).

### 3.2 The accuracy of the interpolation scheme

Here we discuss the numerical accuracy of the interpolation method we employ. For a fixed wavelength we precompute the specific intensity for set of  $(T_{\text{eff}}, \log g, \mu)$  grid points. Given a model combination of  $(T_{\text{eff}}, \log g, \mu)$  we perform a 3-D logarithmic interpolation to determine the specific intensity. Orosz & Hauschildt (2000), showed that the specific intensity values over a given bandwidth are a relatively smooth function of temperature and gravity. We therefore tried linear and cubic spline interpolation methods. In contrast to Orosz & Hauschildt (2000), we found that linear or cubic spline interpolation was not accurate and robust enough, especially towards the limb of the star. Note that we interpolate absorption lines strengths at a given wavelength, whereas Orosz & Hauschildt (2000) interpolate over a large bandwidth. The effects of absorption lines that do not vary smoothly would naturally be smoothed out when integrated over a large bandwidth. The interpolation method we use is based on a modification of Shepards method for a set of 3D scattered data points and is described in Renka (1988). Basically the method computes a smooth trivariate function using an least squares fit to the grid points near the interpolant. This function is then used for the interpolation.

A simple way to test the interpolation scheme is to remove one  $(T_{\text{eff}}, \log g$  and  $\mu)$  grid point from the precomputed intensity grid and then calculate its interpolated value. This

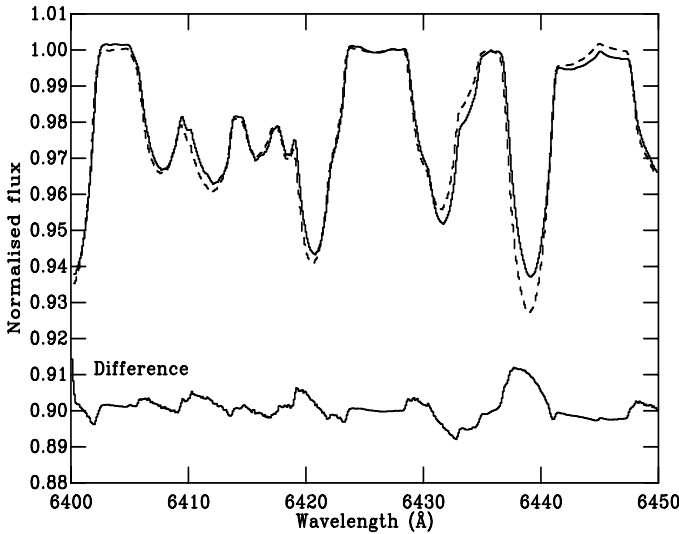


**Figure 1.** The effects of using a limb-darkening law to compute a Roche-lobe model spectrum. The solid line is the high resolution model spectrum (top) where the limb darkening is computed properly. The model parameters are  $q=0.42$ ,  $K_2=215.5 \text{ km s}^{-1}$ ,  $i=70^\circ$ ,  $\beta=0.08$ ,  $\langle T_{\text{eff}} \rangle = 6400 \text{ K}$  and  $\langle \log g \rangle = 4.0$ . The dashed line is the high resolution model spectrum where a linear limb-darkening law has been used with a limb-darkening coefficient of 0.52. The bottom spectrum is the residual spectrum, shifted upwards to clarity.

value can then be compared to the original grid point value and gives an indication of the accuracy of the interpolation method. We compute a normal spectrum where we used all the grid points in the intensity table and a clipped spectrum where we removed the grid point at  $T_{\text{eff}}=4500 \text{ K}$ ,  $\log g=4.5$  and  $\mu=0.10$  from the table. We find the interpolation method to be accurate to <0.5 percent. To determine the effects of using a relatively coarse grid for the Roche-lobe, we computed spectra using two different grids, a standard grid with  $N_\theta=40$  and a fine grid with  $N_\theta=60$ , which corresponds to 2048 and 4194 grid points respectively. We found that the two spectra agreed to within 0.8 percent. Therefore, we believe that our integration and interpolation schemes are accurate to better than 1 percent.

### 3.3 The effects of limb-darkening

We compare two high resolution Roche-lobe model spectra, one where the limb-darkened spectrum is computed properly and the other where the spectrum is computed assuming constant limb darkening (of 0.52) across the line.

In both cases, the same Roche-lobe system parameters are used ( $q=0.42$ ,  $K_2=215.5 \text{ km s}^{-1}$ ,  $i=70^\circ$ , orbital phase=0.35,  $\beta=0.08$ ,  $\langle T_{\text{eff}} \rangle = 6400 \text{ K}$  and  $\langle \log g \rangle = 4.0$ ). In Fig. 1, one can see that the spectra are clearly different. For the constant limb-darkened spectrum, the limb-darkening is assumed to be the same for all the lines. Also, a linear or two-parameter law does not accurately describe the real limb-darkening behavior, since the intensity at the limb of the star is much less (Orosz & Hauschildt 2000). Therefore it is not surprising that the shape and strength of the lines are not the same, especially for the blended lines.

## 4 APPLICATION TO THE SXTS: X-RAY NOVA SCORPII 1994

Due to the faintness of the secondary star in most of the quiescent SXTs, it is usually only possible to obtain intermediate resolution spectroscopy. However, this implies that the shape of the absorption lines cannot be used to determine system parameters (Shahbaz 1998). The only information which we can use is the width of the absorption lines, which is related to  $q$ . To date there are 9 measurements of the binary mass ratio for SXTs (see Table 1), which were all obtained by measuring the secondary star's rotational broadening and using the standard limb-darkened rotation profile. If we are to determine accurate masses for the binary components in the SXTs, we have to try and reduce all known sources of uncertainties. It is possible to eliminate the uncertainties in the binary mass ratio obtained by assuming the standard rotation profile, by determining the true limb-darkened rotationally broadened spectrum of the secondary star. In this section, we outline this method, using the SXT Nova Sco 1994 as an example.

### 4.1 Previous work

The SXT Nova Sco 1994 has been extensively studied over the past years at both X-rays and optical wavelengths [see Shahbaz et al., 1999 (hereafter S99), Orosz & Bailyn 1997 and references within]. Optical photometry taken during X-ray quiescence ( $L_X < 10^{-3} L_{\text{opt}}$ ) revealed the orbital period  $P_{\text{orb}}=2.62168 \text{ days}$  (Orosz & Bailyn 1997). Through modeling the quiescent optical light curves, the binary inclination was measured to be  $70^\circ$  (Orosz & Bailyn 1997). Greene, Bailyn & Orosz (2001) obtained the same result by modeling the optical and infrared quiescent light curves simultaneously with an upgraded code. Spectroscopic observations allowed the radial velocity semi-amplitude to be measured  $K_2=215.5 \pm 2.45 \text{ km/s}$ , which implies a binary mass function of  $2.73 \pm 0.09 M_\odot$  (S99). The spectral type was determined to be F3–F6 (Orosz & Bailyn 1997), and later refined to be F6 (S99).

Since the companion star fills its Roche-lobe and is in synchronous rotation with the binary motion,  $V_{\text{rot}} \sin i$  combined with  $K_2$  gives a direct measurement of  $q$  (Horne, Wade & Szkody 1986)

$$v \sin i = K_2(1+q) \frac{0.49q^{2/3}}{0.6q^{2/3} + \ln(1+q)^{1/3}} \text{ km s}^{-1} \quad (1)$$

S99 used the standard technique to estimate the rotational broadening of the secondary star. Using optical spectra with a velocity resolution of  $38.6 \text{ km s}^{-1}$ , they compared the average observed spectrum of Nova Sco 1994 with field template stars broadened using the standard rotation profile. For limb-darkening coefficients of 0.0 and 0.52, they obtained  $q=0.36$  and  $q=0.40$  respectively. However, it should be noted that the template star they used has an intrinsic rotational broadening of  $\sim 30 \text{ km s}^{-1}$  (see SIMBAD database), which implies that the  $V_{\text{rot}} \sin i$  values were underestimated. In order to determine  $V_{\text{rot}} \sin i$  for Nova Sco 1994, we repeated the analysis described in S99, but using the F6III template star HR5769 ( $V_{\text{rot}} \sin i < 5 \text{ km s}^{-1}$ ; SIMBAD database) and the spectral region  $6380\text{\AA}$ – $6500\text{\AA}$ . For limb-darkening coefficients of 0.0 and 0.52, we obtain  $V_{\text{rot}} \sin i$  values of  $89.6 \pm 2.8$

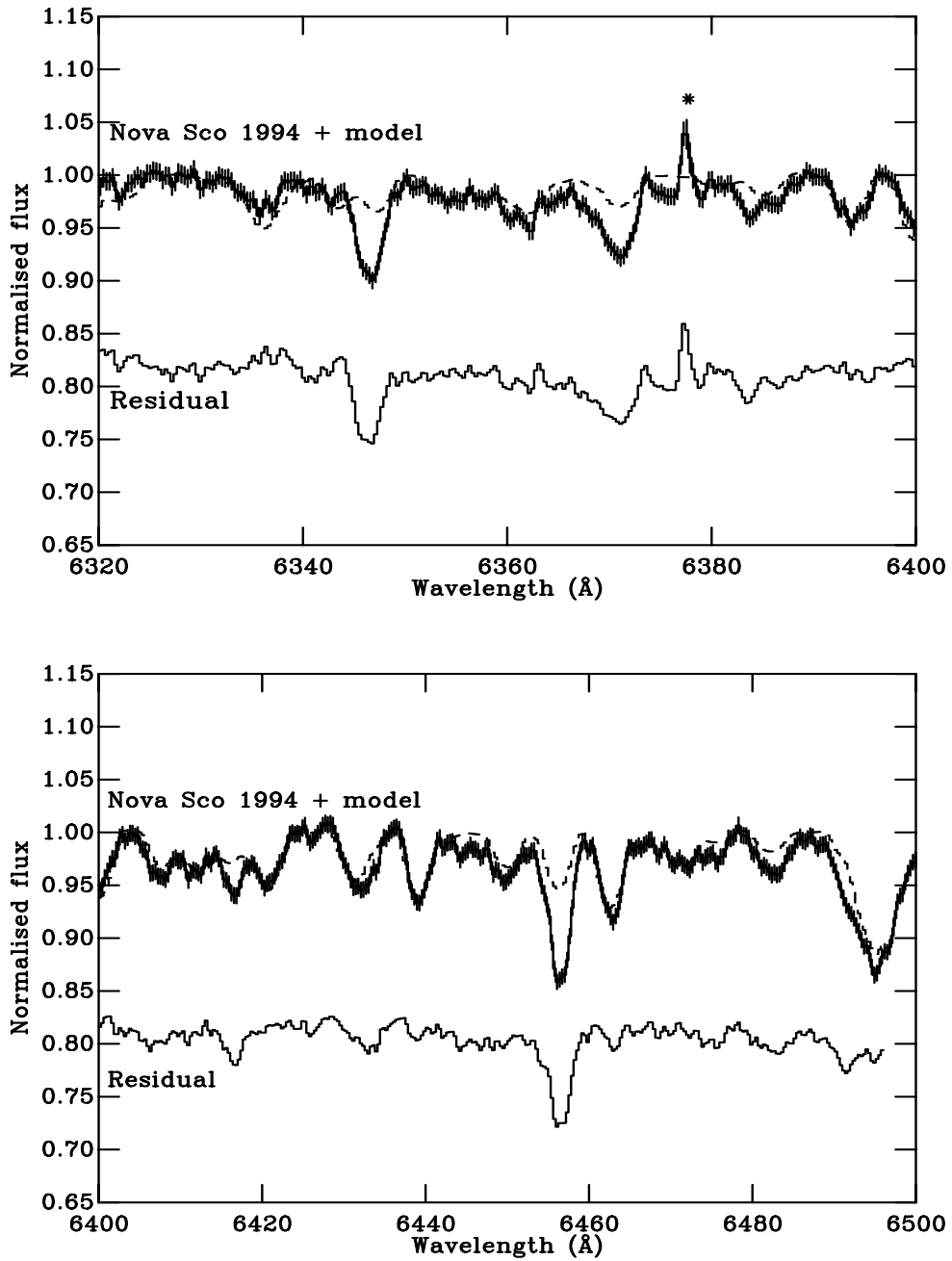


**Figure 2.** The variance-weighted average spectrum of Nova Sco 1994 (solid line) and the best model spectrum overplotted (dashed line) using  $q=0.42$ ,  $i=70^\circ$ ,  $\beta=0.08$ ,  $\langle T_{\text{eff}} \rangle = 6336$  K and  $\langle \log g \rangle = 4.0$ . For the Nova Sco 1994 spectrum we also show the error bars on the data. The residual spectrum of Nova Sco 1994 after subtracting the scaled model spectrum is shown underneath. The feature marked with an asterisk is residual sky line. The spectra have been normalised. All the spectra are in the rest frame of the model.

$\text{km s}^{-1}$   $94.8 \pm 3.0$   $\text{km s}^{-1}$  respectively, which correspond to a mass ratio of  $0.385 \pm 0.023$  and  $0.427 \pm 0.024$  respectively (90 percent uncertainty). We find that the spectrum of the secondary star is not veiled ( $f_v = 1.00 \pm 0.05$ ). These results are consistent with the  $V_{\text{rot}} \sin i$  and veiling values found by Israelian et al., (1999) using high resolution spectra. Note that the difference between the  $V_{\text{rot}} \sin i$  values for Nova Sco 1994 obtained using HR2927 (S99) and HR5769 is  $\sim 20$   $\text{km s}^{-1}$ .

This difference is the rotational velocity of HR2927 and agrees well with the value in the SIMBAD database.

In order to obtain a more accurate determination of  $q$ , which does not depend on assumption about the rotation profile and limb-darkening coefficients, we use the model described in section 3 to compute the exact rotationally broadened model spectrum, which can then be directly compared with the average observed spectrum of Nova Sco 1994 published in S99. Since the Nova Sco 1994 spectra have a res-

olution of  $38.6 \text{ km s}^{-1}$ , we cannot use the shape of the absorption lines to determine system parameters such as  $i$  or  $\beta$  (Shahbaz 1998). The only information which we can use is the width of the absorption lines, which is related to  $q$ .

#### 4.2 Model parameters

In our model, the temperature distribution across the secondary star is described by a gravity darkening law. For stars with radiative atmospheres the exponent ( $\beta$ ) for the gravity darkening law is 0.25 (von Zeipel 1924), whereas if the atmosphere of the star is convective, the exponent is 0.08 (Lucy 1967). The spectral type of the secondary star in Nova Sco 1994 (F6) is on the boundary between hot stars with radiative envelopes and cool stars with convective envelopes. Claret (2000) has shown that the value for  $\beta$  is a function of the star's effective temperature. For Nova Sco 1994 with  $\langle T_{\text{eff}} \rangle = 6336 \text{ K}$ ,  $\beta = 0.08$ . However, to be conservative in our model computations, we use  $\beta = 0.08$  and 0.25.

We fix  $i$  to be  $70^\circ$  (Greene et al., 2001) and assume the secondary to be a F6IV (S99) with an  $\langle T_{\text{eff}} \rangle = 6336 \text{ K}$  and  $\langle \log g \rangle = 4.0$  (Gray 1992). For  $\beta = 0.08$  the temperature and gravity across the secondary star ranges from 5120 K to 6490 K and  $\log g = 2.8$  to 4.1 respectively. The temperature distribution for  $\beta = 0.25$  is much wider and flatter (3230 K to 6780 K) and there is no difference in the range of  $\log g$ .

For a compromise between speed and resolution, we choose the number of grid points to be such that the maximum radial velocity difference between any two adjacent elements is less than the instrumental resolution. We choose the total number of surface elements to be 2048 ( $N_{\theta} = 40$ ; see section 3), which with the binary parameters of Nova Sco 1994, gives a maximum radial velocity difference of less than  $10 \text{ km s}^{-1}$ .

#### 4.3 The binary mass ratio

Our analysis was performed in the same way as by S99, the only difference being that we compute broadened spectra using our model which depends on  $q$ , instead of using broadened template stars. For a given value for  $q$  we first computed the model spectrum in the wavelength range 6300 Å to 6500 Å. This region was chosen since it is similar to the region used in the analysis of S99 and has many relatively isolated absorption line features. We then broadened the model spectrum using a Gaussian function with a width 38.6 km/s to match the instrumental resolution of the Nova Sco 1994 data. We determined the velocity shift of the average observed spectrum of Nova Sco 1994 with respect to the model spectrum using the method of cross-correlation (Tonry & Davis 1979). Prior to the cross-correlation all the spectra were rebinned onto a logarithmic wavelength scale with a pixel size of  $14.5 \text{ km s}^{-1}$ .

In order to compare our model spectrum with the average observed Nova Sco 1994 spectrum, one should compute the model spectra in the same way as the Nova Sco 1994 spectra were obtained and averaged. The Nova Sco 1994 average spectrum consisted of 25 velocity-corrected spectra taken during 2 nights covering orbital phases near 0.35 and

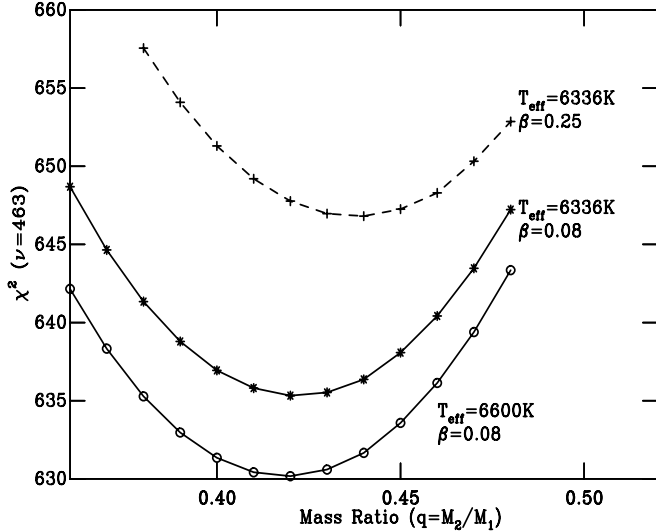


**Figure 3.** The  $\chi^2$  values for the optimal subtraction as a function  $q$ . The stars and crosses show the  $\chi^2$  values for fits using  $\beta=0.08$  and 0.25 respectively with  $\langle T_{\text{eff}} \rangle = 6336 \text{ K}$ . The circles show the  $\chi^2$  values for fits using  $\langle T_{\text{eff}} \rangle = 6600 \text{ K}$  and  $\beta=0.08$ . The minimum  $\chi^2$  is 618.6 and the curve has been shifted upwards.

0.85. Ideally one should compute model spectra at the same orbital phases and allow for the orbital smearing due to the exposure time. However, the resolution of the data is such that any information about the shape of the absorption lines is smeared out (Shahbaz 1998). Therefore, we compute a single model spectrum at phase 0.35 and assume it is the same for all orbital phases.

To allow for the smearing of the absorption lines due to the motion of the secondary star during the length of each exposure at each orbital phase, we convolved the model spectrum with a rectangular function with the appropriate velocity width which is given by  $2\pi K_2 \cos(2\pi\phi)/P_{\text{orb}} \text{ km s}^{-1}$ . We first normalise using a continuum spline fit and then average the 25 model spectra. Finally, to compare the average model spectrum with the average observed spectrum of Nova Sco 1994 we used the method described in Marsh et al., (1994). We subtract a constant,  $f_v$ , multiplied by the model spectrum from the average observed Nova Sco 1994 spectrum. The constant represents the fractional contribution of the template star spectrum to the total flux density. Therefore  $1-f_v$  is the veiling factor and for no veiling  $f_v=1.0$ . The optimum value for  $f_v$  was obtained by minimising the  $\chi^2$  statistic. We performed the above analysis for  $q$  in the range 0.32 to 0.452 in steps of 0.01 and in the wavelength range 6310–6490 Å. The residual sky feature at 6376 Å was masked. We obtain a minimum  $\chi^2$  of 1729.1 ( $\nu=530$ ) at  $q=0.42$ . In Fig. 2 we show the best model spectrum with  $q=0.42$ , the average observed spectrum of Nova Sco 1994 and the residual spectrum. The poor fit is primarily due to the feature at 6346 Å and 6456 Å contributing significantly to the poor  $\chi^2$ . Masking out these features we obtain a minimum  $\chi^2$  of 635.3 ( $\nu=463$ ,  $\beta=0.08$ ). Fig. 3 shows the  $\chi^2$  plot for different values of  $q$ . For the models with  $\beta=0.08$  (circles) the minimum  $\chi^2$  is obtained at  $q=0.422 \pm 0.028$  with  $f_v=0.88 \pm 0.04$  (90 percent uncertainty). Using a gravity darkening exponent of  $\beta=0.25$  (crosses), we obtain a significantly higher  $\chi^2$ ; the

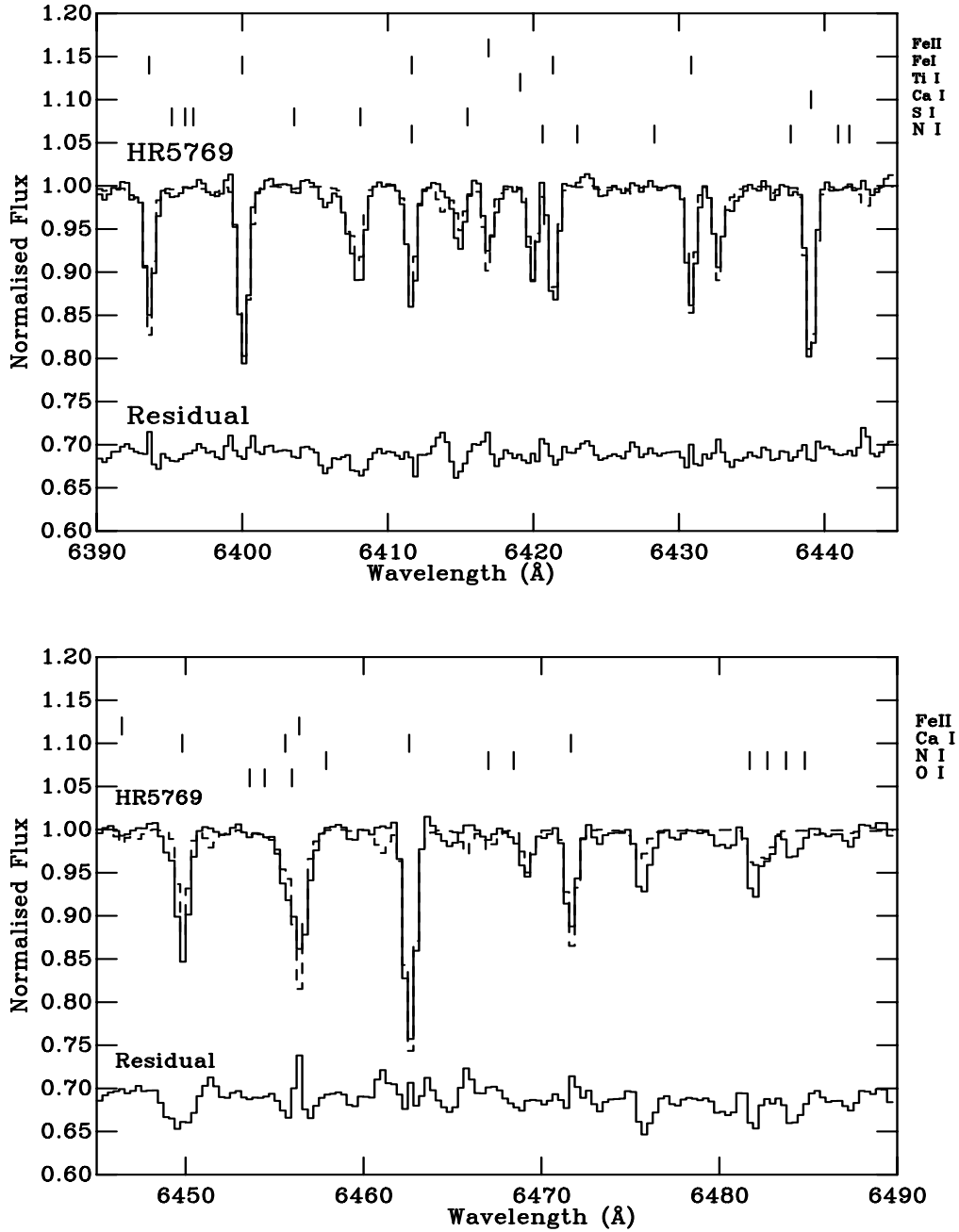


**Figure 4.** The template F6IV star HR5769 (solid line) and the NEXTGEN model spectrum (dashed line) computed using  $T_{\text{eff}}=6400$  K and  $\log g=3.7$  and degraded to match the resolution of the template star spectrum. The residual spectrum is also shown at the bottom. The spectra have been normalised. The wavelength position of the atomic Fe lines and the  $\alpha$ -elements are also shown.

minimum  $\chi^2$  is 646.6 at  $q=0.439\pm0.028$  with  $f_v=0.89\pm0.04$  (90 percent uncertainty).

From optical spectroscopy, S99 and Israelian et al., (1999) showed that there is no evidence that the light from the secondary star is veiled (see also section 4.1). From our fits using  $\langle T_{\text{eff}} \rangle=6336$  K and  $\beta=0.08$  we obtain  $f_v=0.88$ , i.e. the model predicts deeper absorption lines compared to the data. Since our analysis mainly uses Fe absorption lines, which are stronger in cooler stars, we expect by using a hotter secondary star in the model we will obtain a

higher value for  $f_v$ . Using  $\langle T_{\text{eff}} \rangle=6600$  K and  $\beta=0.08$  we obtain a minimum  $\chi^2$  of 618.6 with  $f_v=1.00$ , i.e. the secondary star contributes all the flux. The minimum  $\chi^2$  is at  $q=0.419\pm0.028$  (90 percent uncertainty). A star with  $\langle T_{\text{eff}} \rangle=6600$  K would have an F3 spectral type (Gray 1992), which is consistent with the observed spectral type (F3–F6; Orosz & Bailyn 1997 and S99).

It should be noted that, although the minimum  $\chi^2$  obtained using  $\langle T_{\text{eff}} \rangle=6600$  K is significantly lower than the minimum  $\chi^2$  obtained using  $\langle T_{\text{eff}} \rangle=6336$  K, it should

**Table 2.** Summary of model fits. 90 percent uncertainties are given

Nova Sco 1994	Standard profile		
	u=0.00	$q=0.385 \pm 0.023$	
	u=0.52	$q=0.427 \pm 0.024$	
Nova Sco 1994	Roche profile		
	$\langle T_{\text{eff}} \rangle = 6336 \text{ K}, \beta=0.08$	$q=0.422 \pm 0.028$	
	$\langle T_{\text{eff}} \rangle = 6600 \text{ K}, \beta=0.08$	$q=0.419 \pm 0.028$	
Simulation ( $q=0.42$ )	Standard profile		
	u=0.00	$q=0.392 \pm 0.006$	
	u=0.52	$q=0.434 \pm 0.006$	

be noted that the shape and position of the minimum  $\chi^2$  does not change; the  $\chi^2$  values are only offset by a constant amount. Also, for a fixed  $\langle T_{\text{eff}} \rangle$  the fits using  $\beta=0.25$  give higher values for  $f_v$  compared to the fits using  $\beta=0.08$  (see above). Therefore the determination of  $q$  and its uncertainty does not depend on the choice of  $\langle T_{\text{eff}} \rangle$ . If we use an inclination of  $68^\circ$  or  $72^\circ$ , or if we change  $K_2$  by  $4 \text{ km s}^{-1}$  (the 90 percent limits on  $K_2$ ; see S99) the derived value for  $q$  does not change; the minimum  $\chi^2$  increases by less than 1. Note that the uncertainties in the temperature/spectral type and in  $\beta$  are of the same order as that introduced by using the standard rotational profile.

#### 4.3.1 Overabundant $\alpha$ -elements

The poor minimum  $\chi^2$  we originally obtained before masking can be explained either in terms of the NEXTGEN models failing to reproduce the strength of some of the absorption line features used in the optimal subtraction or that the Nova Sco 1994 spectrum contains some overabundant elements. To see if this mismatch is due to the former, we compare a NEXTGEN model spectrum with a F6IV template star spectrum. The NEXTGEN model spectrum was computed using  $T_{\text{eff}}=6400 \text{ K}$  and  $\log g=4.0$ , values appropriate for the template star HR5769. The model parameters were  $f=0.1$  (i.e. for a spherical star),  $K_2=0.0 \text{ km s}^{-1}$  and  $\beta=0$ . From Fig. 4 it can be seen that we have confidence that our code matches the absorption line features: the scatter in the residual of the lines is less than 2 percent.

Israeli et al., (1999) have measured the metal abundances of the secondary star in Nova Sco 1994 and find  $[\text{Fe}/\text{H}]=0.1 \pm 0.2$  which is consistent with being solar. They also found an overabundance in the  $\alpha$ -elements (O, Ca, S, Mg, Si, Ti and N) compared to solar values. Since the spectral region we use in the optimal subtraction is dominated by Fe lines the use of synthetic models with solar abundances seems correct. We would then naturally expect the few  $\alpha$ -element absorption line features present in the spectral region used for our analysis to be overabundant and hence contributes significantly to the poor  $\chi^2$ . To determine the qualitative effects of the  $\alpha$ -elements abundances, we compare a solar abundance spectrum and a spectrum where the  $\alpha$ -element abundances have been increased, with the observed Nova Sco 1994. (Fig. 5). The abundances of the latter spectrum were increased by  $[\text{O}/\text{H}]=1.0$ ,  $[\text{S}/\text{H}]=0.75$ ,

$[\text{Mg}/\text{H}]=0.9$ ,  $[\text{Si}/\text{H}]=0.9$ ,  $[\text{Ti}/\text{H}]=0.9$  and  $[\text{N}/\text{H}]=0.45$  (Israeli et al., 1999). As Israeli et al., (1999) did not determine the Ca abundance, we also increased the Ca abundance by  $[\text{Ca}/\text{H}]=1.0$  to see if the mismatched feature at  $6456 \text{\AA}$  is due to Ca. Both spectra were computed using  $T_{\text{eff}}=6400 \text{ K}$  and  $\log g=4.0$  and were broadened by  $V_{\text{rot}} \sin i=95 \text{ km s}^{-1}$  using the standard rotation profile ( $u=0.52$ ). Subtracting solar- and enhanced-abundance spectra from the observed Nova Sco 1994 spectrum, we obtain  $\chi^2_{\nu}$  values of 2.95 and 4.15 respectively. The residual solar- and enhanced-abundance spectra are shown in Fig. 5. The mismatched feature at  $6436 \text{\AA}$  contain the  $\alpha$ -elements MgII 6346.742  $\text{\AA}$  and Si 6415.48  $\text{\AA}$ , whereas the feature at  $6456 \text{\AA}$  contains CaI 6455.598  $\text{\AA}$  and OI 6455.977  $\text{\AA}$  but note that FeII 6456.38  $\text{\AA}$  is also present.

While our spectra seem to show that some of the mismatched features are due to the  $\alpha$ -elements being overabundant, there are also a few features that the non-solar spectrum predicts to be overenhanced. To some extent this explains why the  $\chi^2_{\nu}$  for the enhanced spectrum is higher than the  $\chi^2_{\nu}$  for the solar spectrum. Given the poor resolution of the spectra, it is difficult to determine with certainty if the mismatched features are entirely due to the  $\alpha$ -elements being overabundant. Only a more detailed abundance analysis using high resolution spectra can prove this convincingly.

## 5 DISCUSSION

### 5.1 The mass ratio and black hole mass

Beer & Podsiadlowski (2002) determined  $q$  by fitting the optical light curves of Nova Sco 1994 in a self consistent manner, without any assumptions about the distance or interstellar reddening. They obtained  $q=0.256 \pm 0.039$  which is significantly lower than the values obtained by S99 (see also section 4.1) and Greene et al., (2001). They argue that the high mass ratio obtained by Greene et al., (2001) is a consequence of neglecting the accretion disc when modeling the optical and infrared light curve. Furthermore, in order to explain the disagreement in  $q$ , they suggested that the secondary star's rotational broadening measured by S99 was overestimated. [Note that the revised determination of  $q$  (see section 4.1) does not affect the argument presented by Beer & Podsiadlowski (2002)]. They comment that since the spectra in S99 were taken at quadratures near orbital phases 0.25 and 0.75 (orbital phase 0.0 is defined as superior conjunction of the secondary star) the effects of orbital smearing would be the greatest. The orbital smearing would add a linear amount of  $3.5 \text{ km s}^{-1}$  to the rotational broadening. As S99 did not take into account the effects of orbital smearing, the rotational broadening value obtained by S99 would be overestimated.

Firstly, we would like to point out that the effects of orbital smearing would be the least because the velocity of the secondary star is least at the quadratures. Secondly, because the velocity width of the rectangular smearing profile is much smaller than the rotational broadening, the effects of orbital smearing is very small. To examine the effects of orbital smearing on the rotational broadening we performed a simple simulation where we computed a Gaussian function with  $\text{FWHM}=100 \text{ km s}^{-1}$ , appropriate for the observed

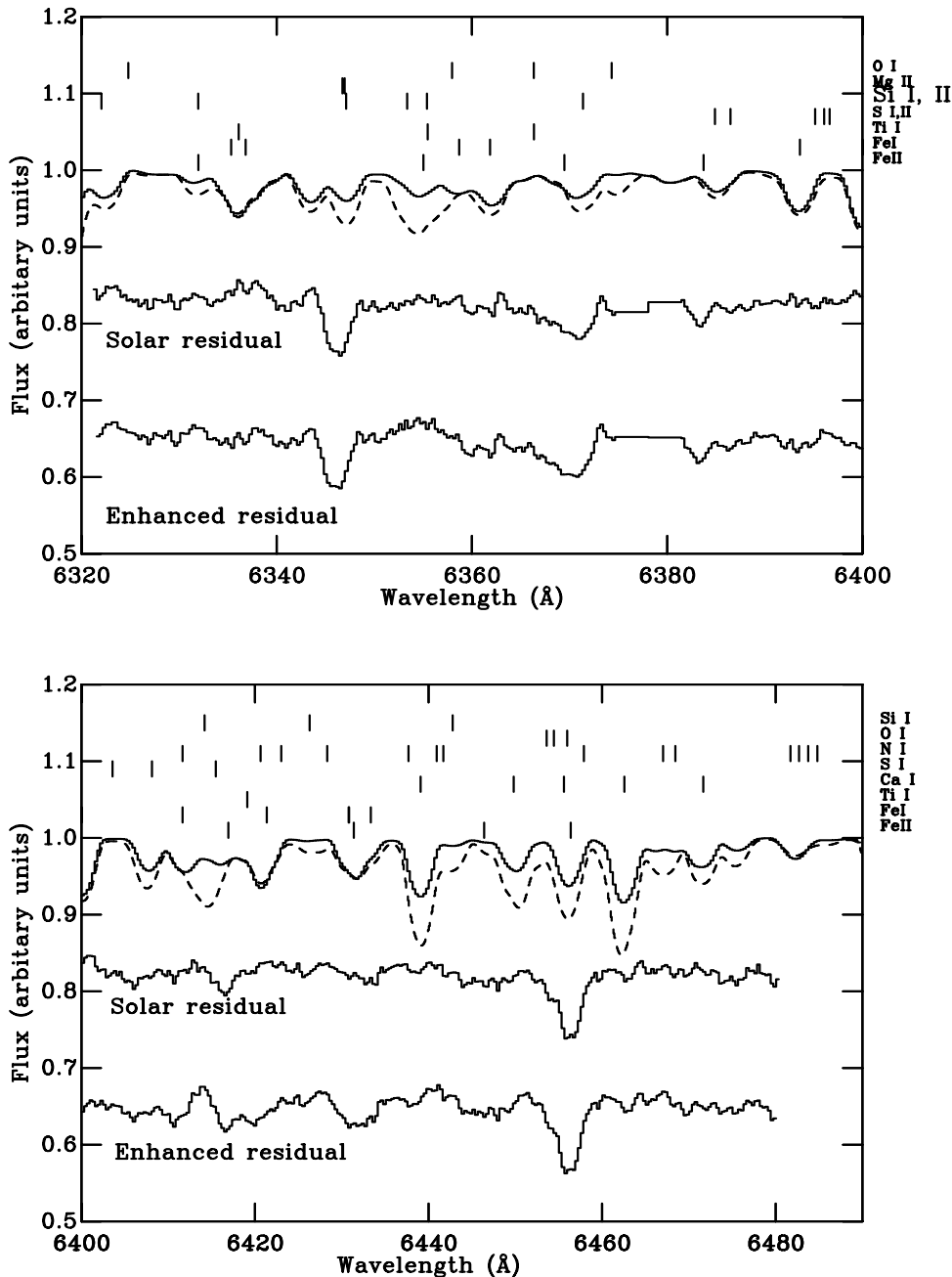


**Figure 5.** A comparison between a solar and non-solar LTE spectrum. The LTE synthetic spectrum were computed with  $\langle T_{\text{eff}} \rangle = 6400$  K and  $\log g = 4.0$ . The solid line shows the LTE spectrum with solar abundance. The dashed lines shows the LTE spectrum where the  $\alpha$ -elements have abundances of  $[\text{O}/\text{H}] = 1.0$ ,  $[\text{S}/\text{H}] = 0.75$ ,  $[\text{Mg}/\text{H}] = 0.9$ ,  $[\text{Si}/\text{H}] = 0.9$ ,  $[\text{Ti}/\text{H}] = 0.9$ ,  $[\text{N}/\text{H}] = 0.45$  (Israelian et al., 1999) and  $[\text{Ca}/\text{H}] = 1.0$ . The LTE model spectra have been broadened by  $95 \text{ km s}^{-1}$ . The residual spectrum after subtracting the solar (middle) and enhanced-abundance (bottom) model spectrum from the observed Nova Sco 1994 spectrum are also shown.

$V_{\text{rot}} \sin i$  (see Royer et al., 2002 for a rule of thumb calibration) and then smeared it with a rectangular profile with a width of  $7 \text{ km s}^{-1}$ . We find that the width of the Gaussian function before and after the smearing is the same to within 0.2 percent, therefore, the effects of orbital smearing are negligible. Also, it should be noted that Beer & Podsiadlowski (2002) obtained  $T_{\text{eff}} = 6150$  K which is significantly different to what we obtain (see section 4.3). Given the sys-

tematic uncertainties in modeling the light curves (e.g. the binary inclination is correlated with  $T_{\text{eff}}$ ) it is difficult to explain the difference in  $q$  obtained by Beer & Podsiadlowski (2002).

Using our value for the binary mass ratio, we can determine the mass of the binary components from the mass function equation

$$f(M) = \frac{PK_2^3}{2\pi G} = \frac{M_1 \sin^3 i}{(1+q)^2} M_{\odot} \quad (2)$$

With  $f(M)=2.73 \pm 0.15 M_{\odot}$  (S99),  $q=0.419 \pm 0.028$  (see section 4.3) and  $i=70.2 \pm 1.6^{\circ}$  (Greene et al., 2001), we obtain  $M_1=6.59 \pm 0.45 M_{\odot}$  and  $M_2=2.76 \pm 0.33 M_{\odot}$ . The 90 percent uncertainties were obtained using a Monte Carlo procedure. Although the the absolute value for the binary mass ratio obtained by Greene et al., (2001) and in this paper are different, the uncertainties in the mass ratio are such that the black hole mass we obtain is consistent with that obtained by Greene et al., (2001).

## 5.2 Roche-lobe versus standard rotation profile

In S99 we determined  $q$  for Nova Sco 1994 by comparing the average observed spectrum of Nova Sco 1994 with the spectrum of a template star which had been convolved with the standard rotation profile. The standard rotation profile requires a limb-darkening coefficient which we assume to be the value appropriate for the continuum i.e. we assume that the radiation in the lines is the same as for the continuum. Since the absorption lines in early type stars will have core limb-darkening coefficients much less than the values appropriate for the continuum (Collins & Truax 1995), in order to be conservative we also used a limb-darkening coefficient of zero. Using a non-rotating template star with line limb-darkening coefficients of zero and 0.52 (note that 0.52 is actually the continuum value), we obtained mass ratio's of  $q=0.385$  and  $0.427$  respectively (see section 4.1). Using the Roche-lobe model we obtained  $q=0.419$  (see section 4.3). As one can see, the Roche-model gives a mass ratio that lies in between the values obtained using limb-darkening coefficients of zero and 0.52 (continuum) and the standard rotation profile.

To prove this, we simulate a spectrum and then try to determine  $V_{\text{rot}} \sin i$  and hence  $q$  in the same way as we did in S99 (see section 4.3) and using the X-ray binary model (section 4.1). We first perform the same analysis as in S99 to determine  $V_{\text{rot}} \sin i$ , i.e. we compare broadened versions of the non-rotating template star HR5769 with the simulated average spectrum, using the standard rotation profile with a continuum limb-darkening coefficients of 0.0 and 0.52. The high quality (S/N=500) model spectrum was computed using  $q=0.42$ ,  $K_2=215.5 \text{ km s}^{-1}$ ,  $i=70^{\circ}$ ,  $\beta=0.08$ ,  $\langle T_{\text{eff}} \rangle=6400 \text{ K}$  and  $\langle \log g \rangle=4.0$ . For limb-darkening coefficients of 0.0 and 0.52 we obtain mass ratio's of  $q=0.392$  and  $0.434$  respectively (90 percent uncertainty of 0.006). Using the binary model, we find that we recover the exact model  $q$  value. These simulations confirm that, for the case of an F-type secondary star, the standard rotation profile with zero and continuum value for the line limb-darkening coefficient gives a value for  $q$  that brackets the value found using the X-ray binary model.

The limb-darkening coefficient varies across the absorption having the continuum value in the wings to a reduced value in the line core, where the exact value for the line limb-darkening coefficient depends on the atomic species of the line. Since most of the absorption in the rotationally broadened line comes from the line core, the value for the limb-darkening in the line core will dominate the shape of the line (Collins & Truax 1995). The fact that we obtain

a better estimate for  $q$  using a limb-darkening coefficient slightly less than the continuum value suggests that the average line limb-darkening coefficient for the strongest absorption lines used in the analysis (i.e. Fe) is close to the continuum value. It is clear that only detailed line profile calculations on individual lines can determine the true absorption line limb-darkening coefficient.

## 6 CONCLUSIONS

We present a model that predicts the spectrum of the secondary in an interacting binary. The model uses synthetic NEXTGEN model spectra which are incorporated into the secondary star's Roche geometry. As a result, we determine the exact rotationally broadened spectrum of the secondary which does not depend on assumptions about the rotation profile and limb-darkening coefficients.

As an example, we determine the mass ratio for the SXT Nova Sco 1994. We use our model to compute the rotationally broadened model spectrum, which we compare directly with the observed intermediate resolution spectrum of Nova Sco 1994. In order to match the width of the absorption lines and the lack of veiling in the quiescent optical spectrum, our model requires  $q=0.419 \pm 0.028$  (90 percent uncertainty), and a secondary star with  $\langle T_{\text{eff}} \rangle=6600 \text{ K}$  (an F3 star) which is consistent with the observed spectral type. For the case of an F-type secondary star, we find that the standard rotation profile with zero and continuum value for the line limb-darkening coefficient gives a value for  $q$  that brackets the value found using the full geometrical treatment.

## ACKNOWLEDGMENTS

I am deeply grateful to Peter Hauschildt for computing the NEXTGEN synthetic spectra. I would also like to thank the referee for the careful reading of the manuscript and for the extremely useful comments that improved the paper. TS was supported by an EC Marie Curie Fellowship HP-MC-CT-199900297.

## REFERENCES

- Allen C.W., 1973, *Astrophysical Quantities*, Athalone Press, London.
- Beer M., Podsiadlowski Ph., 2002, MNRAS, 331, 351
- Casares J., Charles P.A., 1994, MNRAS, 271, L5
- Casares J., Martin E.L., Charles P.A., Molaro P., Rebolo R., 1997, NewA, 1, 299
- Claret A., 2000, A&A, 359, 289
- Collins II G.W., Truax R.J., 1995, ApJ, 439, 860
- Gray D.F., 1992, in *The observation and Analysis of Stellar Photospheres*, Cambridge Astrophys. Ser. 20, Cambridge University Press, Cambridge
- Harlaftis E., Horne K., Filippenko A.V., 1996, PASP, 108, 762
- Harlaftis E., Collier S., Horne K., Filippenko A.V., 1999, A&A, 341, 491
- Hauschildt P.H., Allard F., Baron E., 1997, ApJ, 512, 377
- Hauschildt P.H., Allard F., Ferguson J., Baron E., Alexander D.R., 1999, ApJ, 525, 871
- Horne K., Wade R., Szkody, 1986, MNRAS, 219, 791

Israeli G., Rebolo R., Basri G., Casares J., Martin E.L., 1999,  
*Nat*, 401, 142

Kurucz R.L., 1979, *ApJS*, 40, 1

Linnell A.P., Hubeny I., 1994, *ApJ*, 434, 738

Lucy L.B., 1967, *Z. Astrophysik*, 65, 89

Linnell A.P., Hubeny I., 1996, *ApJ*, 471, 958

Marsh T.R., Robinson E.L., Wood J.H., 19994, *MNRAS*, 266, 137

Orosz J.A., Bailyn C.D., 1997, *ApJ*, 477, 876

Orosz J.A., Hauschildt P.H., 2000, *A&A*, 364, 265

Orosz J.A., Kuulkers E., van der Klis M., McClintock J.E., Garcia M.R., Callanan P.J., Bailyn C.D., Jain R.K., Remillard R.A., 2001, *ApJ*, 555, 489

Orosz J.A., Groot, P.J., van der Klis, M., McClintock J E., Garcia M R., Zhao P., Jain R.K., Bailyn C.D., Remillard R.A., 2002, *ApJ*, 568, 845

Press W.H., Teukolsky S.A., Vettering V.T., Flannery B.P., 1992, in *Numerical Recipes in Fortran*, 2nd edition, Cambridge University Press, Cambridge

Renka R.J., 1988, Algorithm 661: QSHEP3D: Quadratic Shepard method for trivariate interpolation of scattered data, *ACM Trans. Math Software*, 14, 151

Royer F., Gerbaldi M., Faraggiana R., Gmez A.E., 2002, *A&A*, 381, 105

Shahbaz T., 1998, *MNRAS*, 298, 153

Shahbaz T., van der Hooft F., Casares J., Charles P.A., van Paradijs J., 1999, *MNRAS*, 306, 89 (S99)

Shepard D., 1968, A two dimensional interpolation for irregularly spaced data, *Proc. 23rd Nat. Conf. ACM Brandon/Systems Press Inc, Princeton*, 517

Tonry J., Davis M., 1979, *AJ*, 84, 1511

Torres M.A.P., Casares J., Martinez-Pais I.G., Charles P.A., 2002, *MNRAS*, 334, 233

Tjemkes A.S., van Paradijs J., Zuiderveld E.L., 1986, *A&A*, 154, 77

Von Zeipel H., 1924, *MNRAS*, 84, 655

Welsh W.F., Horne K., Gomer R., 1995, *MNRAS*, 275, 649